DEUTSCHES ELEKTRONEN-SYNCHROTRON DESY

DESY SR-82-15
September 1982

SPECTROSCOPIC INVESTIGATION OF THE ELECTRONIC STRUCTURE OF THE CHLORINE MOLECULE

by

Thomas Moeller, Bernhard Jordan, Peter Gürtler and Georg Zimmerer

II. Institut für Experimentalphysik der Universität Hamburg

Dieter Haaks

FB Physikalische Chemie der Universität-GHS Wuppertal

Jacques Le Calve

Centre d'Etudes Nucleaires, Département de Physico-Chimie, Gif-sur-Yvette

Marie-Claude Castex

Laboratoire des Interactions Moléculaires et des Hautes Pressions du C.N.R.S., Centre Universitaire Paris-Nord, Villetaneuse

NOTKESTRASSE 85 · 2 HAMBURG 52

To be sure that your preprints are promptly included in the
HIGH ENERGY PHYSICS INDEX ,
send them to the following address (if possible by air mail) :

DESY
Bibliothek
Notkestrasse 85
2 Hamburg 52
Germany

DESY SR-82-15
September 1982

SPECTROSCOPIC INVESTIGATION OF THE ELECTRONIC STRUCTURE OF THE CHLORINE MOLECULE

Thomas MOELLER, Bernhard JORDAN, Peter GÜRTLER and Georg ZIMMERER
II. Institut für Experimentalphysik der Universität Hamburg,
D-2000 Hamburg 50, Germany

Dieter HAAKS
FB Physikalische Chemie der Universität-GHS Wuppertal
D-5600 Wuppertal, Germany

Jacques LE CALVE
Centre d'Etudes Nucleaires, Département de Physico-Chimie,
91190 Gif-sur-Yvette, France

and
Marie-Claude CASTEX
Laboratoire des Interactions Moléculaires et des Hautes Pressions
du C.N.R.S., Centre Universitaire Paris-Nord, 93430 Villetaneuse, France

Abstract

Vacuum ultraviolet absorption spectroscopy and fluorescence analysis under selective optical excitation have been combined to deduce the electronic structure of Cl_2. Between 73000 cm^{-1} and 81000 cm^{-1} five bound electronic states could be analysed. Some of them are affected by pronounced Rydberg-valence mixing. Especially the $1\,^1\Sigma_u^+$ state clearly yields a double well structure which results from an avoided crossing between an ionic valence and a Rydberg state. The double well structure is responsible for an irregular vibrational sequence between 73000 cm^{-1} and 74500 cm^{-1} which either prevented an analysis in earlier investigation or lead to wrong assignments. The FC factors of $1\,^1\Sigma_u^+$ fluorescence with its bound-bound and bound-free contributions between $\sim$73000cm^{-1} and 50000 cm^{-1} are also severely affected by the double well structure. The results are compared with the first ab initio calculations of the electronic structure of Cl_2. In general, excellent agreement is found.

1. Introduction

Apart from the X $^1\Sigma_g^+$ ground state and B $^3\Pi(0_u^+)$, the electronic structure of the chlorine molecule is known only in fragments [1] . This is especially true in the vacuum ultraviolet spectral range (VUV). Early absorption studies in the VUV yielded a lot of vibrational structure indicating the existence of bound excited states [2] . An unambiguous classification into different progressions together with the extraction of potential curves was not possible. Early VUV fluorescence studies indicated a complex nature of the spectra [3] and enabled only a precise determination of the ground state [4, 5] .

This unsatisfactory situation is partly due to experimental difficulties in VUV spectroscopy with aggressive gases. In view of this paper another reason has to be mentioned. Peyerimhoff and Buencker recently showed that strong Rydberg-valence configuration mixing leads to many avoided crossings of the potential curves and thus to double well potentials with irregular vibrational progressions which cannot be analysed in a simple way [6] .

The electronic structure of Cl_2 received a great deal of attention recently. Cl_2 plays a significant role in rare gas monohalide laser systems [7] and may even be an important laser molecule by its own [8] . These aspects stimulated our first investigations of the dynamics of excited states [9, 10] as well as the first ab initio calculations of the electronic structure of Cl_2 [6] . Two recent high resolution spectroscopic studies by Le Calvé et al. [11] and Douglas [12] improved our knowledge considerably. Rotational analysis enabled a safe determination of the symmetry of several excited states. A few vibrational progressions could be assigned. However, due to the irregularities mentioned above, a safe interpretation of several features was impossible even in the case of Douglas' experiment [12] who used isotope clean chlorine $^{35}Cl_2$. Additional information on some dipole forbidden Rydberg states was obtained from threshold electron impact experiments [13] .

In this paper we present a high resolution absorption study between 73000 cm^{-1} and 81000 cm^{-1} combined with fluorescence analysis between 50000 cm^{-1} and 75000 cm^{-1}. Investigation of VUV fluorescence under state selective excitation is very helpful for a safe interpretation of several absorption features which could not be assigned by Le Calvé et al. [11] and Douglas [12] . It turns out that excitation spectra of the integrated fluorescence differ markedly from absorption spectra. Comparison of both is a key for a better understanding of the electronic structure. We concentrate on the lowest dipole allowed excited state, 1 $^1\Sigma_u^+$, and the effects introduced by its double well structure. Attention is also given to the 2 $^1\Pi_u$ state which dominates in absorption between 74000 cm^{-1} and 77000 cm^{-1}, and to the 2 $^1\Sigma_u^+$ state with its relatively steep potential well which is a result of an avoided crossing (78000 cm^{-1} - 80000 cm^{-1}).

The nomenclature used throughout this paper is taken from ref. [6] . In the tables, the assignments to the states listed in ref. [1] are given whenever possible.

2. Experiment

The experiments were performed at the new synchrotron radiation laboratory HASYLAB at Hamburg [14] . Most of the fluorescence and medium resolution absorption experiments were carried out with an experimental station described in detail elsewhere [15] . Absorption was measured with a band pass of 1.2 Å. Fluorescence was excited with a band pass of 5 Å and analysed with a VUV monochromator (band pass 15 Å). The pressure of Cl_2 in a gas cell with LiF windows ranged between 0.5 torr and 10 torr. All measurements were made at room temperature on natural Cl_2.

When the gross features of the spectra were known we continued our investigation at the new high intensity beam line with its high flux high resolution VUV - 2m - normal incidence monochromator [16] and the new experimental station SUPERLUMI for VUV fluorescence studies under synchrotron radiation excitation [17] . The band pass in absorption was

improved to 0.07 Å. Fluorescence was excited with a band pass of 0.5 Å and analysed with 5 Å resolution. Gas pressure was lowered to 0.1 torr. In view of the short radiative lifetimes of the states under discussion [10] , this pressure practically ensures collision-free case. Whereas the spectral distribution of exciting light was taken into account to deduce the absorption cross-section as a function of energy, the fluorescence spectra are not corrected for the detector response function and the transmission characteristics of the analysing monochromator. For the convolution of both characteristics including different optical elements we expect a continuous decrease in sensitivity with decreasing fluorescence wavelength. The estimated curve is included below. The error in the high energy region may be of the order of a factor of 2 ...3. Therefore, one should not compare fluorescence intensities over a large wavelength interval. This is not necessary within this paper.

3. Results and discussion

3.1 Some remarks on the electronic structure of Cl_2

In fig. 1 we present potential curves of the Cl_2 molecule in order to facilitate the following discussion. The X $^1\Sigma_g^+$ ground state with its $\sigma_g^2 \pi_u^4 \pi_g^4 \sigma_u^0$ configuration was taken from ref. [5], because this is - to the best of our knowledge - the most accurate determination presently available. From the manifold of repulsive or weakly bound states terminating at Cl $^2P_{3/2}$ or $^2P_{1/2}$ atoms, we included the well established $^3\Pi(0_u^+)$ state [18] and the 1 $^1\Pi(1_u)$ state which is responsible for a broad absorption band centered around 32000 cm^{-1} [19] .

The curves in the upper part of fig. 1 all stem from ref. [6] (ab initio calculation, spin orbit splitting being neglected). The lowest bound $^1\Sigma_u^+$ valence states are of ionic nature, terminating at $Cl^+(^1D_g)$ + $Cl^-(^1S_g)(\sigma_g \rightarrow \sigma_u)$, and at $Cl^+(^1S_g)$ + $Cl^-(^1S_g)$ $(\pi_u \pi_g \rightarrow \sigma_u^2)$. Their equilibrium distances (2.7 - 3 Å) are considerably larger than r_o = 1.9879 Å of the ground state. Around 2.1 Å and 2.4 Å, respectively, they cross the lowest $^1\Sigma_u^+$ Rydberg state ($\pi_g \rightarrow 4p\pi$). Due to strong configuration mixing, in the adiabatic limit, two double well states result,

namely 1 $^1\Sigma_u^+$ and 2 $^1\Sigma_u^+$. The inner well of 1 $^1\Sigma_u^+$ is very shallow, whereas the inner well of 2 $^1\Sigma_u^+$ is deep and considerably steeper than the ground state. The outer wells mainly reflect the shapes of the ionic precursors.

The adiabatic 2 $^1\Pi_u$ state obtains its double well structure from an avoided crossing of a $\pi_g \rightarrow 4p\sigma$ type Rydberg state (terminating at $Cl(^2P_u)$ + $Cl^*(^2D_u, 4p)$) and a $\pi_u \pi_g \rightarrow \sigma_u^2$ valence state terminating at $Cl^+(^1D_g)$ + $Cl^-(^1S_g)$. The outer well, however, is outside the FC region and thus does not influence the absorption spectra. Its inner well turns out to cause the most prominent absorption features between 74000 cm^{-1} and 77000 cm^{-1}, whereas the inner well of 2 $^1\Sigma_u^+$ governs absorption between 78000 Å and 81000 Å. For all of these states we expect a strong change of the electronic transition moment passing the internuclear distance of the avoided crossing region which is supported by preliminary theoretical results [20] .

In fig. 1, the notation used by Peyerimhoff and Buenker has been taken. In reality, however, an intermediate coupling between Hund's coupling cases (a) and (c) is more realistic [21, 22] . In the text, whenever necessary, the notation of case (a) is used.

3.2 Absorption between 73000 cm^{-1} and 77000 cm^{-1}

In fig. 2, the absorption cross-section (in arbitrary units) of natural Cl_2 is given between 73000 cm^{-1} and 77000 cm^{-1}. Included are the positions of three vibrational progressions I,II and III which have been identified by Douglas [12] and Le Calvé et al. [11] for $^{35}Cl_2$. Excellent agreement can be stated. We are able to identify additional members of the progressions and clearly see the isotope shift between $^{35}Cl_2$ and $^{35}Cl^{37}Cl$. ($^{37}Cl_2$ is not identified due to its small abundance in natural Cl_2). Numerical results are listed in table 1. The resolution of 0.07 Å is still not good enough for a rotational analysis. Therefore, we take the position of the maxima of the envelopes as a measure for the transition energies.

Between 73000 cm^{-1} and 74500 cm^{-1} the spectrum cannot at all be explained by the three progressions alone. There exist several extra peaks. Around 74000 Å they have a completely irregular sequence. The assignment given in fig. 2 will be discussed below. It indicates the contribution of $^{35}Cl_2$. The peaks left are mainly due to $^{35}Cl^{37}Cl$ (details in sec. 3.4).

Consulting the ab initio calculations of Peyerimhoff and Buenker [6] for interpretation we note that only two optically allowed states, namely the 1 $^1\Sigma_u^+$ and the 2 $^1\Pi_u$ state exist in the energy range of interest (fig. 1). The 1 $^1\Sigma_u^+$ state is expected to yield strong irregularities due to its double well structure and thus cannot account for the most prominent progression I which is nearly regular. We ascribe progression I to the 2 $^1\Pi_u \rightarrow X\ ^1\Sigma_g^+$ transition. This interpretation is supported by the rotational analysis of the 0-0 transition by Douglas which yielded a $\Pi - \Sigma$ structure [12] . From the energetic positions of the five members which are observed we deduce the vibrational quantum, ω_e, and the anharmonicity factor, given in table 1. The observed isotope splitting agrees well with the values calculated from the reduced masses.

Our Cl_2 VUV spectra are the first from which not only energetic positions but also intensity information is obtained. So we are able to deduce the internuclear distance of the minimum of the 2 $^1\Pi_u$ potential curve. With the parameters given in ref. [5] ($X\ ^1\Sigma_g^+$) and in table 1 (2 $^1\Pi_u$) the FC factors were calculated and fitted to experiment. Optimal agreement was obtained with $r_0 = 1.90$ Å which is slightly smaller than the groundstate value and thus explains why the bands under discussion are blue shaded. In the calculation, r-independent transition moments were assumed which is reasonable in view of the fact that we are not in a region of an avoided crossing.

In table 1 we also compare our results with the calculations of Peyerimhoff and Buenker [6] . The calculated energy difference between the minima of $X\ ^1\Sigma_g^+$ and 2 $^1\Pi_u$ agrees within less than 1 % with the measured energy of the 0-0 transition.

In ref. [6] , the vibrational quantum of 2 $^1\Pi_u$ was not calculated. However, the molecular data of the convergence limit, $Cl_2^+(^2\Pi_g)$, which belongs to the 2 $^1\Pi_u$ Rydberg state are given. ω_e of $Cl_2^+(^2\Pi_g)$ agrees well with our measured value.

For an assignment of progressions II and III, the only candidates are the 0_u^+ and 1_u components of the $\pi_g \rightarrow 4p\sigma\ ^3\Sigma_u$ state which has also been calculated [6] . Its potential curve is practically parallel to the one of 2 $^1\Pi_u$ but lower in energy (fig. 1). The calculated energetical difference of the minima of $X\ ^1\Sigma_g^+$ and 2 $^3\Pi_u$ (70600 cm^{-1}) is considerably lower than the energy of the 0-0 transitions of both progressions. Our assignment is in qualitative agreement with the threshold electron impact excitation experiment of Jureta et al. [13] who found no excitation between 68500 cm^{-1} and 72500 cm^{-1}, but strong signals above 72500 cm^{-1} due to the $4p\sigma\ ^{3,1}\Pi_u$ manifold.

3.3 UV and VUV fluorescence of Cl_2

The fluorescence features of Cl_2 in the UV and VUV spectral range depend strongly on the energy of exciting light. State selective excitation is indispensable in understanding the spectra. Details will be discussed in a forthcoming paper [23] . Here we give a few examples of fluorescence and excitation spectra which turned out to be the key for the analysis of irregular absorption features below 74500 cm^{-1} (1 $^1\Sigma_u^+$ progression in fig. 2).

Fig. 3 shows two fluorescence spectra of 0.5 torr Cl_2 obtained with slightly different excitation energies (upper curve 73440 cm^{-1}, lower curve 73560 cm^{-1}, fwhm $\sim$ 25 cm^{-1}). Both excitation energies are marked in fig. 2 and in the fluorescence spectra themselves. Fluorescence extends from resonance emission down to $\sim$ 50000 cm^{-1} (additional weak lower energy features [23] being neglected). Due to the very short lifetime of $\sim$ 3 ns found recently [10] , fluorescence stems from a dipole allowed transition. The only candidate for allowed transitions in this energy range is 1 $^1\Sigma_u^+$, especially its outer well. The 1 $^1\Sigma_u^+ \leftrightarrow X\ ^1\Sigma_g^+$ differential potential shows that the low energy range of fluorescence ($\sim$ 50000 cm^{-1} - 55000 cm^{-1}) is dominated by outer well bound-free transitions [23] .

In this energy range, a close similarity between both spectra of fig. 3 is found. Above 55000 cm^{-1} the vibrational structure of the ground state is identified. The FC factors for bound-bound transitions in this energy yield a peculiar behaviour, namely a systematic sequence of weak and strong transitions ($v'' \gtrsim 6$. Details will be given in ref. [23]). The positions of $v' \rightarrow v''$ transitions included in fig. 3 are calculated with ω_e and $\omega_e x_e$ of the ground state given in ref. [1] .

Drastic differences between both spectra are found in the region of $0 \leq v'' \leq 6$. In the upper curve strong emission is found here. Emission is weak in the lower curve. It turns out that this different behavior reflects a different nature of the emitting state, one being more concentrated in the inner well, the other one more in the outer well of $1\ ^1\Sigma_u^+$.

Of great importance for an understanding of the absorption features in the spectralrange under discussion are excitation spectra of the spectrally integrated fluorescence. One example is shown in fig. 4 (resolution 0.5 Å, pressure 0.5 torr). Its overall shape differs markedly from the absorption curve which is included for comparison. Low energy peaks which are weak in absorption are strongly enhanced in the excitation spectrum.We can identify nearly all of the red shaded Σ-Σ type transitions of $^{35}Cl_2$ which have been analyses by Le Calvé et al. [11] and by Douglas [12] in this energy range (bars in fig. 4). Of course, our spectrum contains many additional peaks due to $^{35}Cl^{37}Cl$.

The most prominent progression in absorption, $2\ ^1\Pi_u \leftarrow X\ ^1\Sigma_g^+$, is practically absent in the excitation spectrum. Obviously, $2\ ^1\Pi_u$ does not decay radiatively but pre-dissociates via potential curve crossing with repulsive states correlated to ground state atoms. This explains its diffuse nature found in absorption [12] .

In the energy range of fig. 4, pre-dissociation can be excluded only for the outer well $1\ ^1\Sigma_u^+$, because the crossing take place at shorter internuclear distances [6] . Taking in mind the symmetry analysis [11,12] , this immediately made us to assign the low energy features of the excitation spectrum to direct outer well $1\ ^1\Sigma_u^+ \leftarrow X\ ^1\Sigma_g^+$ transitions.

In the inner well region, the probability for pre-dissociation is a sensitive function not only of FC factors but also of the details of the coupling which is adequate to characterise the states. For inner well $1\ ^1\Sigma_u^+$ and the excited states of progressions II and III, pre-dissociation cannot be totally allowed, because rotational analysis was possible [11,12] . However, pre-dissociation may contribute to the decay. From excitation spectrum we conclude that it exceeds fluorescence in the case of progressions II and III, but is of minor importance for inner well $1\ ^1\Sigma_u^+$. In the next section it will be shown that the excitation spectrum can be explained nearly quantitatively by $1\ ^1\Sigma_u^+ \leftarrow X\ ^1\Sigma_g^+$ transition. In other words, it is a measure for the $1\ ^1\Sigma_u^+$ partial absorption cross-section.

3.4 Contribution of $1\ ^1\Sigma_u^+ \leftarrow X\ ^1\Sigma_g^+$ transitions to absorption and excitation spectra

In order to estimate the contribution of the $1\ ^1\Sigma_u^+$ state to absorption and excitation spectra, the FC factors were calculated. The measured ground state potential curve [5] was approximated by a Hulburt-Hirschfelder potential [24] . This seems to be justified because no high vibrational levels, where the usual model potentials are no good approximations [5] , are involved.

For the excited state none of the usual model potentials could be used due to the double well structure. The potential given by Peyerimhoff and Buenker [6] was approximated by an analytical expression which is essentially a superposition of a Morse potential ($\sim$ inner well) and a combination of a Coulombic and a modified Morse potential ($\sim$ outer well) with weighting factors which are a function of internuclear distance. The weighting functions look complicated because a continuous modelling of the potential hump between the inner and the outer well was to be achieved. Details are given in table 2.

For both potentials, Schrödinger's equation was solved following the mathematical procedure described in ref. [25] . In fig. 5, the vibrational levels and some selected eigenfunctions of $1\ ^1\Sigma_u^+$ are shown. As expected, the vibrational spacing gets irregular in the energy range of the double well. Below the inner well, the wavefunctions are restricted to the outer

well region (see, e.g., v' = 35). In the energy region of the inner well, closely spaced in energy, states exist which are either restricted more to the inner well (e.g. v' = 37) or more to the outer well (v' = 38). The molecule can tunnel from the inner well to the outer well and vice versa. All calculations were carried out only for the $^{35}Cl_2$ isotope.

For a comparison with experiment, the calculation of FC factors must include the r-dependence of the electronic transition moment. We expect a pronounced change at the position of the hump, because here the nature of the excited state changes from covalent to ionic type. In fig. 6 we show the transition moment used in our calculation. It is based on preliminary results of Peyerimhoff and Buenker [20] .

In fig. 4, the calculated FC factors are included as bars. Good agreement with the $^{35}Cl_2$ structures in the excitation spectra concerning (i) the energetic positions and (ii) intensities was obtained after a systematic variation of the parameters of the upper state potential. There are a few exceptions. At 72760.6 cm^{-1} and 72811.3 cm^{-1} Douglas identifies two $^{35}Cl_2$ - bands. The model yields only one transition at 72701 cm^{-1}. A similar situation holds for the region of 74000 cm^{-1} where Douglas identifies three Σ-Σ bands at 73911 cm^{-1}, 73972 cm^{-1} and 74021 cm^{-1}, whereas the model yields two bands at 73922 cm^{-1} and 74054 cm^{-1}. However, the assignment of Douglas' Σ-Σ bands to the 1 $^1\Sigma_u^+$ state of $^{35}Cl_2$ is not unequivocal. In fig. 4, those structures are marked which are characterised by Douglas as "strong" or " medium". Besides them "weak" structures exist for $^{35}Cl_2$ which must be partly due to an additional state perturbing the 1 $^1\Sigma_u^+$ state. Perhaps it is the 0_u^+ component of a $^3\Sigma_u^-$ state below the 1 $^1\Sigma_u^+$ state, terminating at $Cl^+(^3P_g) + Cl^-(^1S_g)$ [2] . This state was not calculated by Peyerimhoff and Buenker and could therefore not be included in fig. 1. Moreover, there is a slight disagreement between Le Calvé et al. [11] and Douglas [12] . Le Calvé et al. only report on a transition at 72761 cm^{-1} where Douglas finds the two transitions mentioned above. Around 74000 cm^{-1} Le Calvé et al. did not give a definite analysis of all transition due to the complexity of the spectra.

In a few cases our model yields vibrational levels where Douglas did not find a band. These are always regions where strong absorption of progressions I, II, or III is found making impossible the analysis of comparatively weak Σ-Σ structures.

In fig. 5 we contrast the original potential curve of ref. [6] and our improved potential. The deviations are small. The position of the inner minimum was shifted by less than 0.1 Å. Its energy agrees within 2 - 3 % with the calculation. The assignment of absorption structures to the 1 $^1\Sigma_u^+$ state of $^{35}Cl_2$ given in fig. 2 is based on the improved potential curve. The remaining peaks in the excitaiton spectrum as well as in absorption are ascribed to the 1 $^1\Sigma_u^+$ state of the other isotopes and to the "weak" Σ-Σ structures mentioned above.

Our improved 1 $^1\Sigma_u^+$ potential is not only supported by the agreement between FC factors and the fluorescence excitation spectrum, but also by the fluorescence spectra themselves. It predicts exactly the different behavior of the spectra shown in fig. 3. The wavefunction of the emitting state of the upper curve is mainly concentrated to the inner well leading to strong emission to $0 \leq v'' \leq 6$ of the ground state. The wavefunction of the other emitting state is mainly localised in the outer well. Consequently, emission to $0 \leq v'' \leq 6$ is weak. Explicit FC factor calculations for fluorescence [23] are in agreement with the fluorescence curves.

From the model we expect that all Σ-Σ bands are red shaded with one exception. The v' = 37 state localised in the inner well should be blue shaded. Indeed, the envelope of the corresponding absorption band is the only one among the Σ-Σ bands in this energy range which is blue shaded. Douglas also found only one blue shaded band in this energy range [12] . In his table 5, it is positioned at 73341 cm^{-1}. At this energy we don't see a band in agreement with Le Calvé et al [11] . On the other hand, Douglas does not mention the blue shaded band found at 73441 cm^{-1} which is the strongest feature in this energy region. We suppose that there is a printing error in Douglas' paper. In fig. 4 we omitted a bar at 73341 cm^{-1} and placed it to 73441 cm^{-1}. Le Calvé et al. [11] report on strong blue shaded absorption around 73440 cm^{-1} but were not able to perform a rotational analysis due to saturation effects.

The double well structure seems to cause a peculiar behavior of the isotope effect. Whereas v' = 37 of $^{35}Cl_2$ is mainly concentrated in the inner well region, its $^{35}Cl^{37}Cl$ counterpart is an outer well state. On the other hand, v' = 38 of $^{35}Cl^{37}Cl$ seems to have a strong inner well contribution, whereas v' = 38 of $^{35}Cl_2$ is more restricted to the outer well. This behavior, however, needs further careful experiments on isotope clean Cl_2.

The absolute numbering of the vibrational levels is based on the depth of the outer well calculated by Peyerimhoff and Buenker [6] . It must be correct within 1 % because it predicts accurately the energetic position of bound free fluorescence features [23] . The error in the absolute numbering is estimated to be at most ± 2.

In table 3 we have summarised numerical results for the $1\ ^1\Sigma_u^+$ state. It must be emphazised that ω_e and $\omega_e x_e$ is only valid for $v' \lesssim 35$ where the influence of the inner well can be neglected. In the measured spectra, however, even in this energy range the sequence of vibrational levels is not really regular. This was already found by Le Calvé et al. [11] and Douglas [12] . The nature of the perturbing state is not known. Perhaps it is the 0_u^+ component of the already mentioned $^3\Sigma_u^-$ state.

Before leaving this section we want to point out an interesting phenomenon. Both the envelope of the FC factors and of the excitation spectrum in Fig. 4 yield an oscillatory behavior with maxima around 73450 cm^{-1}, 73960cm^{-1}, 74450 cm^{-1} and 75200 cm^{-1}. The first maxima correspond to the energetic position of states mainly concentrated in the inner well and may thus be a rough measure of the vibrational quantum of the diabatic Rydberg state $\pi_g \rightarrow 4p\pi\ ^1\Sigma_u^+$ ($\omega_e \sim 500 \ldots 600$ cm^{-1}). The positions of the higher maxima of the envelope would nicely fit into the vibrational progression of the diabatic precursor. It seems as if the envelope were some kind of 'memory' of the adiabatic states to the diabatic parent states.

3.5 Correct ordering of $1\ ^1\Sigma_u^+$ and $^1\Pi_u$

The ab initio calculations [6] yielded a crossing of $1\ ^1\Sigma_u^+$ and $2\ ^1\Pi_u$ in the region of the inner wells, the minimum of $2\ ^1\Pi_u$ being lower than the minimum of $1\ ^1\Sigma_u^+$ (see fig. 1). It was admitted that this finding was not conclusive due to the limited accuracy of the calculations. In fig. 5, for comparison, we have included the $2\ ^1\Pi_u$ potential curve as extracted from our measurements. We now see that the minimum of the Π state is slightly above the minimum of the Σ state.

3.6 Absorption between 77000 cm^{-1} and 81000 cm^{-1}

Fig. 7 displays the absorption cross-section of Cl_2 in this energy range. It is governed by a strong progression. With increasing energy we clearly see the isotope splitting. The rotational envelope gets also more and more pronounced. Numerical results are listed in table 4. The energetic positions of the bands correspond to the maxima in absorption.

The progression is ascribed to $2\ ^1\Sigma_u^+ \leftarrow X\ ^1\Sigma_g^+$. The $2\ ^1\Sigma_u^+$ state is the only candidate in this energy range with such a large vibrational spacing. The calculated energetic difference between both potential curves involved (78250 cm^{-1} [6]) is in excellent agreement with the measured energy of 0-0 transition (78135 cm^{-1}). The vibrational quantum estimated from the ab initio potential curve [6] is in good agreement with measurement. The vibrational progression is not regular, the difference between v' = 0 and v' = 1 being too small.

It was not tried to calculate the position of the minimum of the $2\ ^1\Sigma_u^+$ potential curve as was done in the case of $2\ ^1\Pi_u$ for the following reason. For $2\ ^1\Sigma_u^+$ the intensities are extremely sensitive to the actual r-dependence of the transition moment, because the $2\ ^1\Sigma_u^+$ minimum is a result of an avoided crossing and thus covers the region where the transition moment may change drastically. The value of r_o = 2.1 Å given in table 4 is an estimate based on the experimentally deduced position of the hump of $1\ ^1\Sigma_u^+$.

Besides the 2 $^1\Sigma_u^+$ progression many additional absorption features are found. Part of them can be identified as hot bands (fig. 7). However, there exists an additional progression which is indicated in fig. 7, too. It seems to be split into two components. If this splitting were due to the isotope effect, the 0-0 transition would be considerably lower in energy and outside the range discussed here (around $\sim$ 75000 cm^{-1}). 75000 cm^{-1} is approximately the region of the bottom of 2 $^3\Pi_u$ (see table I). We may speculate that the 0_u^+ component of 2 $^3\Pi_u$ extracts oscillator strength from the 2 $^1\Sigma_u^+$ state when vibrational levels nearly coincide leading to a resurrection of 2 $^3\Pi_u$ (0_u^+) in this energy range. Interaction of both states could also account for the irregularities of the 2 $^1\Sigma_u^+$ progression.

4. Comparison with former results

In the compilation of data on diatomic molecules of Huber and Herzberg [1] only states "M", "N", "O" and "P" are listed for the energy range covered by our experiment. The vibrational progression of "P" which was measured by Lee and Walsh [2] and Iczkowski et al. [26] is obviously identical with progression 1 which was assigned in this paper to 2 $^1\Pi_u \rightarrow X\ ^1\Sigma_g^+$. The improved values for ω_e and $\omega_e x_e$ are not far from those given in ref. 1. The value for r_e is new. A rotational constant could be extracted by Douglas [12] only for v' = 0. The higher members are diffuse.

The vibrational progression "M" [2] is identical with progression III with one important exception. Lee and Walsh [2] positioned the 0-0 transition to 72891 cm^{-1} which can be ruled out definitely in view of the results of [11,12] and of this paper.

The only information on the 0-0 transitions of states "N" and "O" [1] stems from the emission work of Douglas and Hoy [5] who identified J' = 28 and 20 and J' = 14 and 10 rotational levels as emitting states, the electronic nature and vibrational quantum being unknown. In the emission work [4,5], only P and R branches were found. Therefore the unknown state must be a $^1\Sigma$ state. Obviously, the "0-0 transition of N" (73363.3 cm^{-1}) is the head of the red shaded band measured by Douglas at 73363.3 cm^{-1} [12]. In this paper it is identified as v' = 36 of the 1 $^1\Sigma_u^+$ state.

The situation is not so clear with state "O". Near to the band head at 74018.5 cm^{-1} given in ref. [1] Douglas has found the head of a red shaded band at 74021 cm^{-1} which is strongly perturbed so that the rotational constants could be determined only poorly. Huber and Herzberg [1] calculated the bandhead energy at 74018.5 cm^{-1} from the energies of J' = 28 (74167.90 cm^{-1}) and J' = 20 (74095.78 cm^{-1}) with the rotational constant given in ref. [5]. Obviously the strong perturbation of the rotational levels is responsible for the difference between 74018.5 cm^{-1} and 74021 cm^{-1}. Our model assigns the band under discussion to v' = 40 or 41 of the 1 $^1\Sigma_u^+$ state.

5. Concluding Remarks

Cl_2 is one of the few homonuclear diatomic molecules which exist under normal conditions in nature. Nevertheless, in spite of many experimental efforts, this small molecule could keep secret its electronic structure in the VUV range for a long time. The reason is quite obvious now. Strong configuration mixing of valence and Rydberg states leads to pronounced irregularities in the optical spectra.

Many of these irregular features could be disentangled in the present work. The basis for this step forward was twofold. It was (i) the combination of absorption and fluorescence spectroscopy, and (ii) the interplay between experiment and theory. Without the ab initio calculations of Peyerimhoff and Buenker [6] the analysis of the spectra would have been considerably more difficult.

Nevertheless, several features in the optical spectra remain unclear. It is highly desirable to perform ab initio calculations of the triplet states with the same standard as was done with the singlet states. Moreover, spin-orbit coupling etc. should be treated explicitly. A first attempt has been made by Jaffe [27] who calculated (among the excited states) only the ionic valence states including spin-orbit effects. These states are mainly responsible for the fluorescence (and lasing) properties of Cl_2. We suppose that they are also very important for elementary reactions of rare gas atoms (R) with excited Cl_2^* molecules. It was already shown that reactions

of the type $R + Cl_2^* \rightarrow RCl^* + Cl$ are efficient mechanisms for a production of the important rare gas monohalide laser molecules [9]. But the ionic states alone are not sufficient for an understanding of intramolecular dynamics in Cl_2.

In the near future we hope to continue our work on isotope clean $^{35}Cl_2$ at considerably better resolution. The range of excitation energy will be extended to the LiF cut-off. With these improved experimental conditions it will be possible to attack the open questions.

Acknowledgement

The authors wish to thank Professor S.D. Peyerimhoff for numerous valuable discussions during the course of this work. It was helpful to bring the ab initio calculations to our notice prior to publication. One of us (G.Z.) wants to thank Dr. R.L. Jaffe for sending his results prior to publication. The support of our work by the crew of HASYLAB (Hamburg) is gratefully acknowledged. The work was sponsored by the Bundesministerium für Forschung und Technologie of the Federal Republic of Germany.

References

[1] K.P. Huber and G. Herzberg, Molecular spectra and molecular structure, IV. Constants of diatomic molecules (Van Nostrand, New York, 1979) and references given therein.

[2] J. Lee and A.D. Walsh, Transactions of the Faraday Society 55 (1959) 1281

[3] R.K. Asundi and P. Venkateswarlu, Ind. J. Phys. 21 (1947) 76; P. Venkateswarlu, Proc. Ind. Acad. Sci. A26 (1947) 22

[4] Y.V. Rao and P. Venkateswarlu, J. Molec. Spectrosc. 9 (1962) 173

[5] A.E. Douglas and A.R. Hoy, Can. J. Phys. 53 (1975) 1965

[6] S.D. Peyerimhoff and R.J. Buenker, Chem. Physics 57 (1981) 279

[7] e.g. Ch.A. Brau, in: Excimer Lasers, ed. Ch.K. Rhodes, Topics in Applied Physics 30 (Springer-Verlag Berlin/Heidelberg/ New York, 1979) p. 87

[8] C.H. Chen and M.G. Payne, Appl. Phys. Letters 28 (1976) 219; A.K. Hays, Opt. Communic. 28 (1979) 209

[9] M.C. Castex, J. Le Calvé, D.Haaks, B. Jordan and G. Zimmerer, Chem. Phys. Letters 70 (1980) 106

[10] J. Le Calvé, M.C. Castex, D. Haaks, B. Jordan and G. Zimmerer, Il Nuovo Cimento 63B (1981) 265

[11] J. Le Calvé, M.C. Castex, E. Boursey and Y. Le Duff, European Conference on Atomic Physics, Heidelberg 1981, EPS Abstracts 5A, Part I, p. 319, and to be published

[12] A.E. Douglas, Can. J. Phys. 59 (1981) 835

[13] J. Jureta, S. Cvejanović, M. Kurepa and D. Cvejanović, Z. Physik A, 304 (1982) 143

[14] O. Beimgraben, W. Graeff, U. Hahn, J. Knabe, E.E. Koch, C. Kunz, G. Materlik, V. Saile, W. Schmidt, B.F. Sonntag, G. Sprüssel, E.W. Weiner und R. Zietz, Phys. Blätter 37 (1981) 2

[15] U. Hahn, N. Schwentner and G. Zimmerer, Nucl. Instr. Methods 152 (1978) 261

[16] H. Wilcke, W. Böhmer and N. Schwentner, Nucl. Instr. Methods in press

[17] P. Gürtler, M. Pouey, E. Roick and G. Zimmerer, Proc. Internat. Conf. on Synchrotron Radiation Instrumentation, Hamburg 1982, to be published in Nucl. Instr. Methods

[18] J.A.C. Todd, W.G. Richards and M.A. Byrne, Trans. Faraday. Soc. 63 (1967) 2081

[19] P. Sulzer and K. Wieland, Helv. Phys. Acta 25 (1952) 653; G.E. Gibson, O.K. Rice and N.S. Bayliss, Phys. Rev. 44 (1933) 193

[20] S.D. Peyerimhoff and R.J. Buenker, private communication

[21] R.S.Mulliken, Rev. Mod. Phys. 4 (1932) 1

[22] M.A.A. Clyne and D.H. Stedman, Trans. Faraday. Soc. 64 (1968) 1816

[23] T. Moeller, P. Gürtler, G.Zimmerer, D.Haaks, J. LeCalvé and M.C. Castex Proc. 6th Internat. Conf. on Spectral Line Shapes Boulder 1982, to be published

[24] H.M. Hulburt and J.O. Hirschfelder, J. Chem. Phys. 9 (1941) 61

[25] F.Y. Hajj, J. Phys. B: Atom. Molec. Phys. 13 (1980) 4521

[26] R.P. Iczkowski, J.L. Hargrave and J.W. Green, J. Chem. Phys. 33 (1960) 1261

[27] R.L. Jaffe, private communication

Figure captions

Fig. 1 Potential curves of Cl_2 (not complete). Lower part: experimental curves, refs. given in text. Upper part: ab initio calculations of ref. [6]. Dotted curves: diabatic potentials.

Fig. 2 Absorption cross section of Cl_2 as a function of photon energy ($\Delta\lambda$ = 0.07 Å, p = 0.1 torr). The progressions are discussed in the text. The arrows indicate the excitation energies for the fluorescence spectra of fig. 3 (v' = 37 and 38, resp., of $1\ ^1\Sigma_u^+$) Note: The strong peak at v' = 38 which shows up in the spectrum is the 0-0 transition of progression III. v' = 38 of $1\ ^1\Sigma_u^+$ is hidden in the absorption background.

Fig. 3 Two typical fluorescence spectra of Cl_2. Excitation energies are indicated in the figure by arrows. The vibrational quanta of the final state ($X\ ^1\Sigma_g^+$) are indicated in the upper part (correct scale for the upper curve). The dashed curve is a rough estimate of the sensivity function of the analysing system.

Fig. 4 Excitation spectrum of the integrated fluorescence of Cl_2 (lower curve, $\Delta\lambda$ = 0.5 Å). Strong and medium red shaded bands (ref. [12]) are indicated by the lines above the curve.
* see text
Bars below the excitation spectrum: results of model calculations (sec. 3.4). For comparison, an absorption spectrum is included (upper curve, $\Delta\lambda$ = 0.07 Å)

Fig. 5 Comparison between the $1\ ^1\Sigma_u^+$ potential curve extracted from fluorescence excitation spectra and the ab initio calculation of ref. [6] (dashed line). Included are typical wavefunctions (v' = 35, 37, 38) of $1\ ^1\Sigma_u^+$ and the vibrational levels. The $2\ ^1\Pi_u$ potential curve as derived from our absorption measurements is included. The energy scale has its zero point at the bottom of the ground state.

Table 1: Experimental data for progressions I, II, III and comparison with theory, whenever possible. Energies in cm^{-1}, internuclear distances in Å.

progression	I			II			III		
assignment	$2^1\Pi_u \leftarrow X^1\Sigma_g^+$			$2^3\Pi(0_u^+) \leftarrow X^1\Sigma_g^+$			$2^3\Pi(1_u) \leftarrow X^1\Sigma_g^+$		
v' ← v''	$^{35}Cl_2$ a)	$^{35}Cl_2$ b)	$^{35}Cl^{37}Cl$ b)	$^{35}Cl_2$ a)	$^{35}Cl_2$ b)	$^{35}Cl^{37}Cl$ b)	$^{35}Cl_2$ a)	$^{35}Cl_2$ b)	$^{35}Cl^{37}Cl$ b)
0-0	74441.2	74443		74284.2	74283		73531.7	75532	
1-0	75063	75065		74928.04	74928	74898	74150.0	74148	
2-0	75687	75690	75671	75562.88	75558	75539	74764.2	74758	74740
3-0		76296	76270		76182	76152	75366	75364	75340
4-0		76897							
w_e b)		634			653			620	
$w_e x_e$ b)		4			4.5			2.5	
r_o b)		1.91			∿ 1.90			∿ 1.90	
r_o c)	1.94			1.94					
ΔE d,c)	74300			70600					
$X^2\Pi_g(Cl_2^+)$ c)	w_e = 620; r_o = 1.92								
notation in e)	P			missing			M f)		

a) from ref. [12] ; b) this work; c) from ref. [6] ; d) energetic distance between potential curve minima; e) ref. [1] ; f) restrictions see sec. 4.

Fig. 6 Transition moment of $1\ ^1\Sigma_u^+ \leftarrow X\ ^1\Gamma_g^+$ used in the model calculation of sec. 3.4. The r-dependence of the groundstate wavefunction for v'' = 0 is given, too.

Fig. 7 Absorption of Cl_2 at higher energies. The progressions are discussed in text. The scale is the same as in fig. 2. Between 79000 cm^{-1} and 80000 cm^{-1} the baseline is not constant due to fluctuations in the electron beam of the storage ring.

Table 2: Analytical expression for the potential curves used in the model calculations of sec. 3.4 and values of the different parameters.

$X\ ^1\Sigma_g^+$	$V(r) = D_e \{(1-e^{-x})^2 + Cx^3e^{-2x}(1+bx)\}$; $x = 2\beta\ (\frac{r-r_o}{r_o})$
parameters	D_e = 20277 cm^{-1}; β= 1.989; r_o = 1.988 Å; c = 0.2126; b = 1.2121
$1\ ^1\Sigma_u^+$	$V(r) = V_1(r)\ f_1(r) + V_2(r)\ f_2(r) + E_o$ with $V_1(r) = D_e\ (1 - e^{-\beta(r-r_o)})^2$ $V_2(r) = E_1 - \frac{Z}{r} + C\ \{1-e^{-\alpha(r^x(r-r_1))}\}^2 - E_o - C$ $f_1 = \frac{\exp\{(\frac{R}{r})^{25}\} - (\frac{R}{r})^{25} - 1}{\exp\{(\frac{R}{r})^{25}\} - (\frac{R}{r})^{25}}$ $f_2 = \frac{\exp\{(\frac{r}{R})^{25}\} - (\frac{r}{R})^{25} - 1}{\exp\{(\frac{r}{R})^{25}\} - (\frac{r}{R})^{25}}$
parameters	D_e = 20558 cm^{-1}; β = 2.192; r_o = 1.852 Å E_o = 73428 cm^{-1}; E_1 = 108104 cm^{-1}; C = 2410.9 cm^{-1}; Z = 116645 cm^{-1}; r_1 = 3.228 Å; $x = 0.6 + \frac{0.38184}{\ln r}$ α = 0.5238; R = 2.021 Å

Table 3: Comparison between the results of our model calculation and results of absorption studies (only $^{35}Cl_2$). The calculations were made for $J'' = 30$ ($\sim$ maximum of the rotational distribution of the ground state at room temperature). Experimental results are mainly band head energies. Differences between both values are below the general accuracy of the calculation ($\sim \pm 0.5$ %).

v'	energy/cm^{-1} (model)	energy/cm^{-1} a)
28 ± 2	71575	71 749.5
29	803	984.1
30	72030	72 162.7
31	255	370.2
32	479	581.9
33	701	72 760.6 and 72 811.3 (see sec. 3.4)
34	922	976.7
35	73139	73 191.8
36	352	363.3
37	460	341 b) (see also sec.3.4)
38	564	561 (weak)
39	764	754.2
40	934	911
41	74054	74 021 and 73 972 (see sec. 3.4)
42	210	strong II absorption overlaps; 74 230 b)
43	385	334
44	551	475
45	714	615
46	881	strong II absorption overlaps; 74 749 b)
47	75052	75 080 (weak)
48	220	224 (weak)
49	393	390 b)
for v' $\lesssim$ 35: $\omega_e = 243^{+0}_{-10}$ cm^{-1}; $\omega_e x_e \approx 0.33$ cm^{-1}		

a) from ref. [12](only red shaded bands characterized as strong or medium unless otherwise specified).

b) from the excitation spectrum, peak energies or shoulders, this work.

Table 4: Experimental data for progression between 77000 and 81500 cm^{-1}. Energies in cm^{-1}.

progression	$2\ ^1\Sigma_u^+ \leftarrow X\ ^1\Sigma_g^+$		not yet assigned	
$v' \leftarrow v''$	$^{35}Cl_2$	$^{35}Cl^{37}Cl$	$^{35}Cl_2$	$^{35}Cl^{37}Cl$
(0 - 0)	78135		77450	77390 ?
(1 - 0)	79103	79076	78020	77990 ?
(2 - 0)	80080	80045	78662	78607 ?
(3 - 0)	80881	80828	79313 ?	79225 ?
ω_e	1040	1016	79519 [a]	
$\omega_e x_e$	42	39	79833	79735 ?
ω_e [b]	1000		80330 [a]	80275 [a]
$E_{(o-o)}$ [b]	78250 ± 800			
r_o [b]	≈ 2.1 Å			

a) most probably hot bands of $2\ ^1\Sigma_u^+ \leftarrow X\ ^1\Sigma_g^+$

b) from ref. [6].

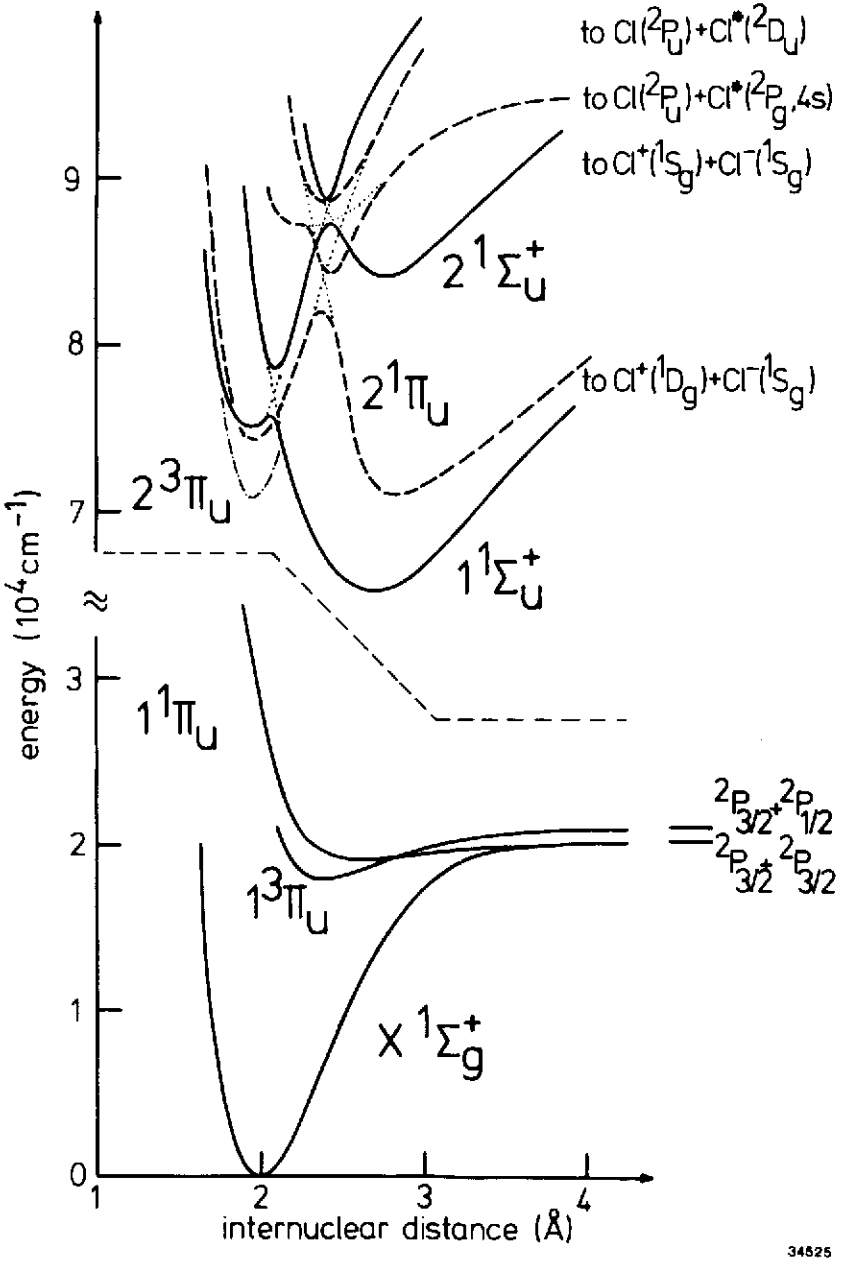

Figure 1

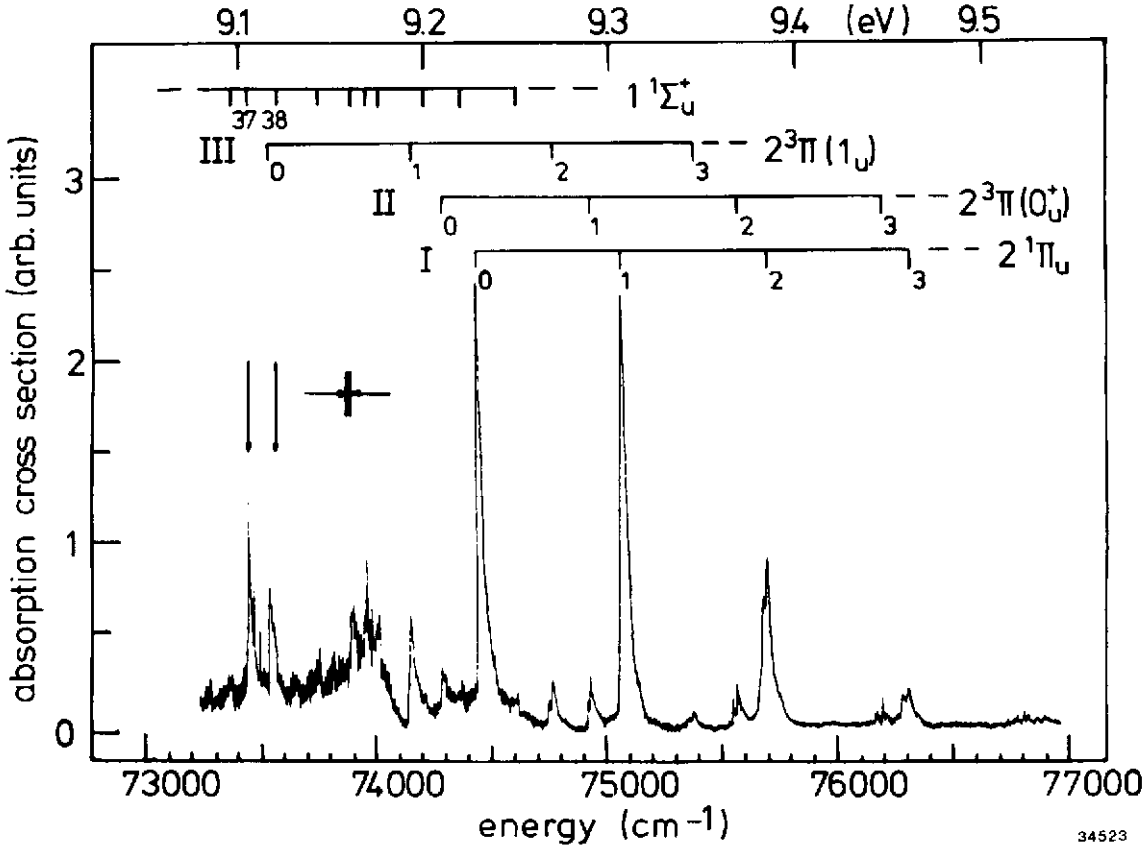

Figure 2

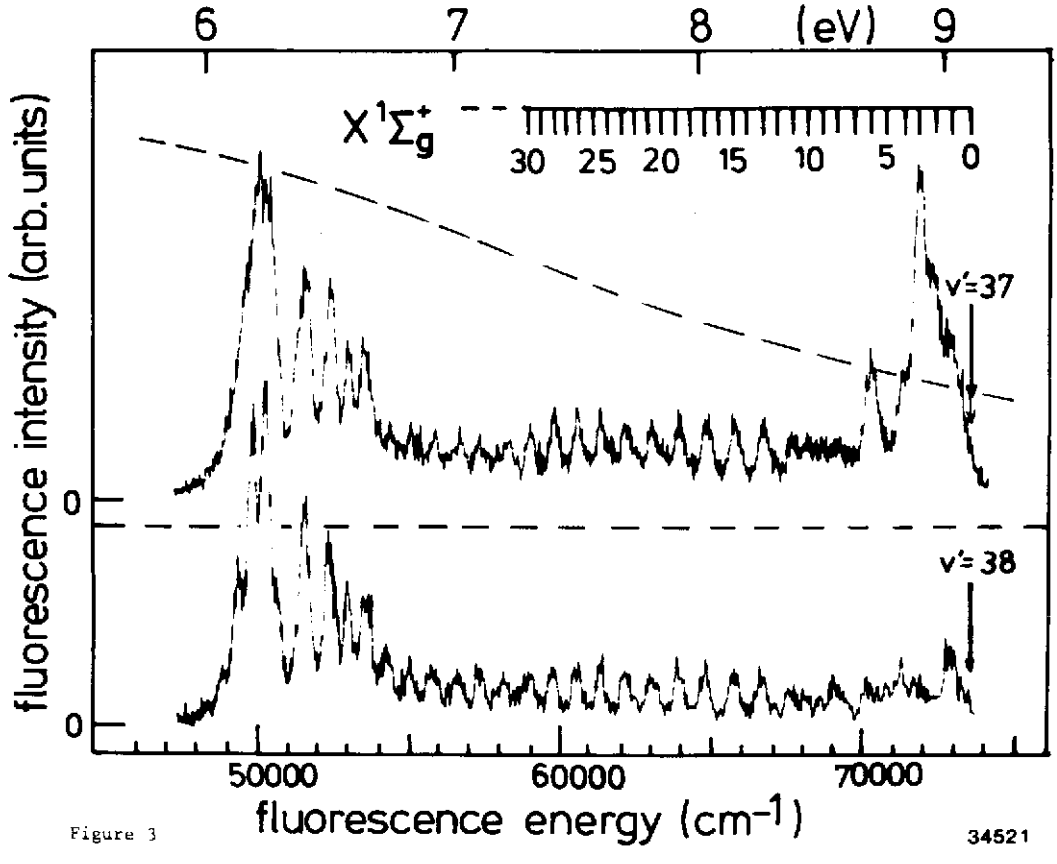

Figure 3

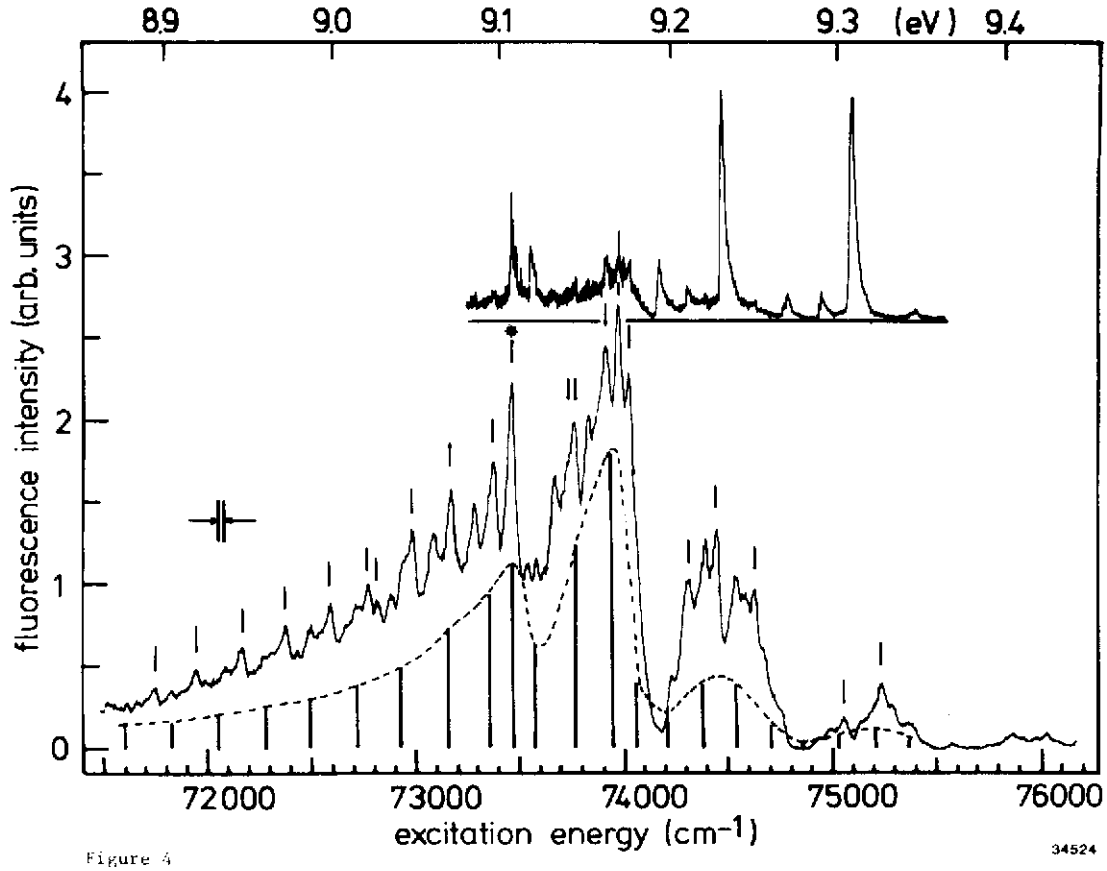

Figure 4

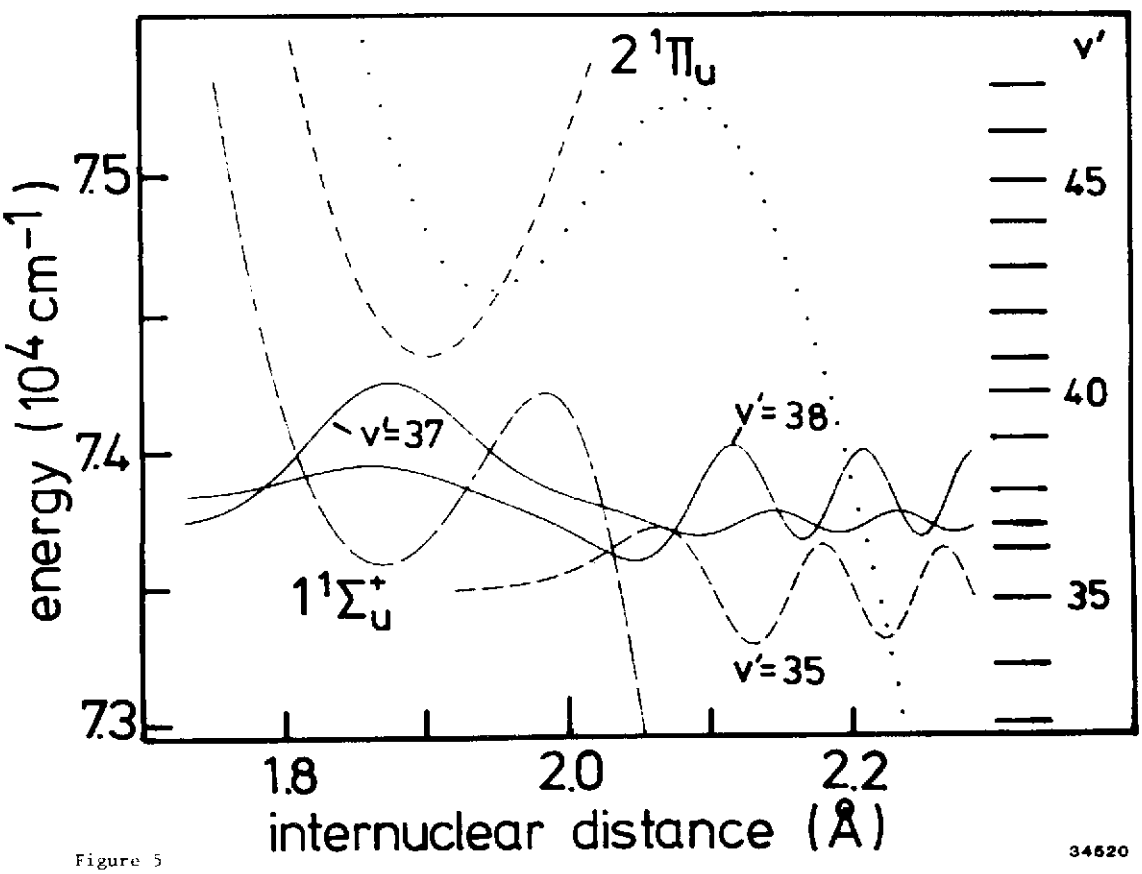

Figure 5

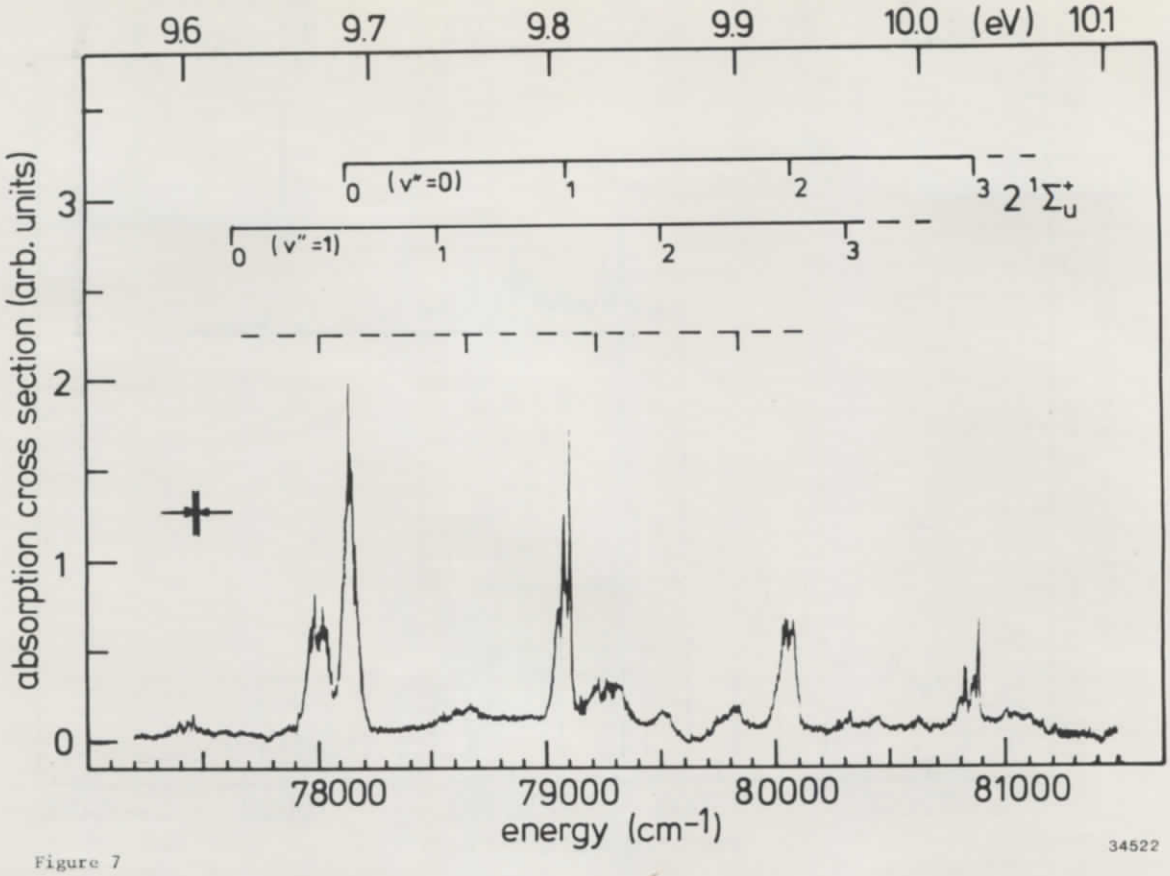

Figure 7

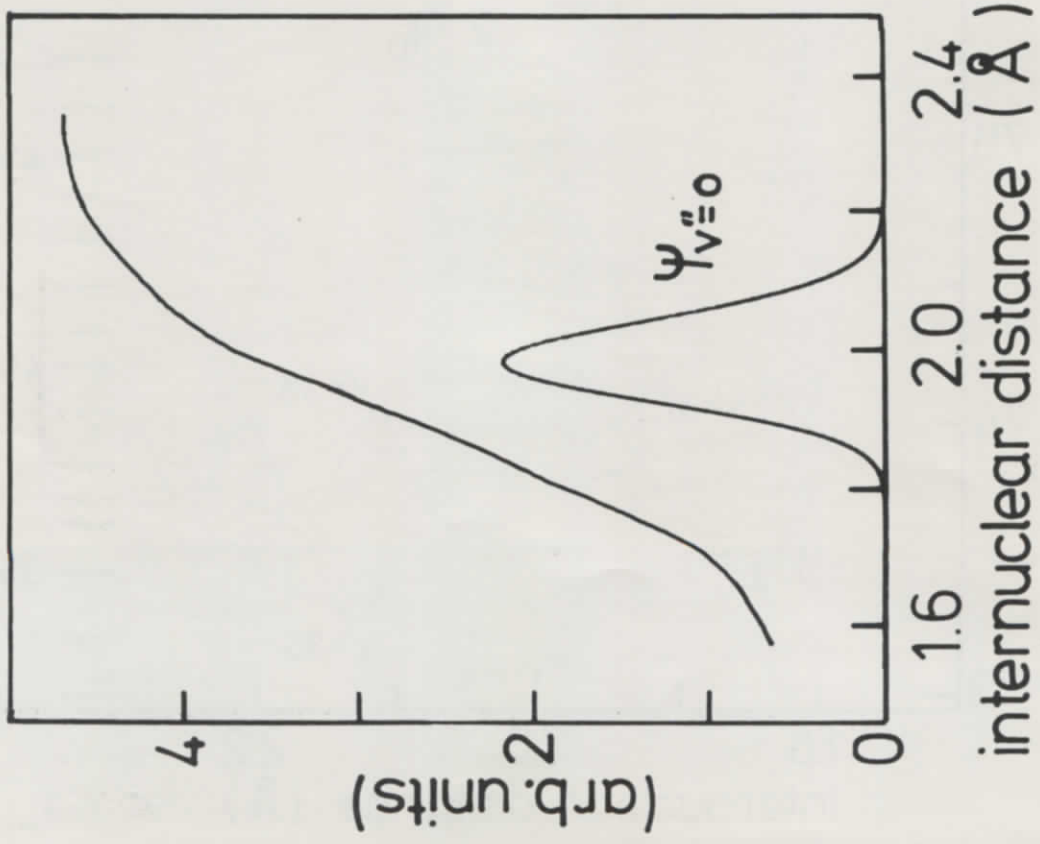

Figure 6